energies

MDPI

Article

Analysis of HT-PEM MEAs' Long-Term Stabilities †

Julian Büsselmann [1,*], Maren Rastedt [1], Tomas Klicpera [2], Karsten Reinwald [2], Henrike Schmies [1], Alexander Dyck [1] and Peter Wagner [1]

1 DLRInstitute of Networked Energy Systems, Carl-von-Ossietzky Str. 15, 26129 Oldenburg, Germany; rastedtmaren@gmail.com (M.R.); henrike.schmies@dlr.de (H.S.); alexander.dyck@dlr.de (A.D.); P.Wagner@dlr.de (P.W.)

2 FUMATECH BWT GmbH, Carl-Benz-Straße 4, 74321 Bietigheim-Bissingen, Germany; Tomas.Klicpera@fumatech.com (T.K.); Karstenreinwald@gmx.net (K.R.)

* Correspondence: Julian.Buesselmann@dlr.de

† This paper is an extended version of our conference proceeding published in 2018 ECS Meeting Abstracts at AiMES Meeting of The Electrochemical Society, Cancun, Mexico, September 30–October 4, ECS Transactions, 86 (13) 301–314 (2018).

Received: 14 November 2019; Accepted: 21 January 2020; Published: 24 January 2020

Abstract: Despite the great advantages of high-temperature polymer electrolyte membrane (HT-PEM) fuel cells over the low-temperature (LT) PEM alternative, such as enhanced reaction kinetics and higher tolerance against impurities like CO due to the higher operation temperature, the achievement of high lifetimes still remains a challenge. In order to improve the durability of the fuel cell, extensive research has been carried out on alternatives for the individual components. For this reason, this paper conducted extended long-term tests with three three membrane electrode assemblies (MEAs) from one manufacturer under different operational scenarios. The MEAs differed mainly by the membranes used and showed significantly different behaviors. While the first MEA reached the end of life already after 2600 h, the second one could pass 9800 h almost without any problems. The third MEA proved resistant to adverse conditions. For all three MEAs, extensive electrochemical characterizations and μ-CT examinations for the analysis of long-term stability are shown.

Keywords: fuel cell; HT-PEM; long-term test; reformate operation

1. Introduction

The goal of the German project QUALIFIX, funded by by the German federal Ministry of Economics and Technology BMWi, is, firstly, to develop common conditions for quality analysis and control for mass production at all levels with manufacturers of an entire value chain of fuel cells and their systems in order to increase the lifetime of fuel cell systems and, secondly, to minimize costly manufacturing losses at an early stage in all production stages. These include the definition of quality requirements as well as the development and provision of suitable test and measurement methods for the production and characterization of membrane electrode assemblies (MEAs), bipolar plates, stacks and, of course, the entire system of a complete power supply unit using the example of a mobile high-temperature polymer electrolyte membrane (HT-PEM) fuel cell power unit, an auxiliary power unit (APU). The strong interest in such a coordinated quality assurance system in the series production of fuel cell components is reflected in the involvement of companies at all stages of the value chain in this project.

In addition to the development of quality control steps to capture relevant product criteria and meaningful test and measurement methods, improving fuel cell components, such as MEAs and membranes, to increase the lifetime of these single cells and fuel cell systems is one of the overarching sublines of this project. This also completes the quality control circle, as durability and stability are the quality features for each type of product including high-temperature polymer electrolyte

membrane fuel cells. Compared with the low-temperature (LT) representatives of this fuel cell type, the degradation rates of HT-PEM fuel cells are higher at the moment [1,2]. Nevertheless, HT-PEM fuel cells are steadily improving [3–5] as shown by Søndergaard et al. [6] with ultra-low degradation rates of 1.4 µV/h and are on the rise, as their higher CO tolerance represents a significant advantage over the LT-PEM fuel cells [7,8]. However, while performance and reproducibility of HT-PEM MEAs generally show a positive tendency, durability under field conditions is still a challenge.

For these reasons, the longevity of MEAs was investigated by means of long-term tests (duration: 1 year) under a constant load of 0.3 A/cm^2 within the framework of QUALIFIX. In addition, qualities of MEAs were reviewed by carrying out small series of evaluations under load cycling conditions at high current densities and start/stop and potential cycling conditions [9–11].

Furthermore, this article also presents long-term test results that are not measured under aspects of the project QUALIFIX but by the project partner and MEA manufacturer FUMATECH BWT GmbH. Thus, three long-term tests are published in this paper which together add up to over 16,000 h of test time (see Table 1). The uniqueness of this work is the comparison of measurements under scientific and industrial aspects with the result that one of the chosen membrane's chemistry withstands both approaches under different stressful conditions.

Table 1. Overview of the tested MEAs, tested at Deutsches Zentrum für Luft- und Raumfahrt (DLR; German Aerospace Center) and Fumatech BWT GmbH (FMT).

MEA	Test Duration	Carried Out At
FMT-A	2700 h	DLR
FMT-B	9800 h	DLR
FMT-C	3850 h	FUMATECH
FMT-X (used as reference material)	1000 h	FUMATECH

2. Materials and Methods

2.1. Membrane Electrode Assembly

All experiments were carried out with commercially available MEAs from the pilot manufacturing plant of FUMATECH BWT GmbH. The MEAs, which were used for long-term testing, had membranes based on polybenzimidazole (PBI) copolymers. The first MEA tested for this publication had a Fumapem® AM-40 membrane, while the second and third adapted MEAs contained a Fumapem® AP-30 membrane. The two membranes' chemistries differed in structure; the AP membrane is a classic type of PBI, while the AM membrane contains in the structure a softening segment allowing very good handling. In addition, the membranes differed in both content of phosphoric acid (i.e., so-called doping level) and doping procedures "in order to achieve the requested high proton conductivity" (p. 1 [12] and [13]). Each membrane was doped with 85 wt% H_3PO_4 in H_2O. Due to the fact of proprietary issues, the exact conductivity target values cannot be given. In the case of the AM-40, doping was carried out at a temperature of 125–135 °C for one hour [14], while the temperature window of 135–140 °C for AP was used; the doping duration of a minimum of 6 h was significantly longer [15]. The platinum loading of the MEAs with a nominal active surface area of 25 cm^2 was set at a constant of 0.55–0.65 mg/cm^2 of platinum (Pt) on anode (Pt/C HS 9100, Johnson Matthey, London, United Kingdom) and 1.6–1.7 mg/cm^2 of Pt on cathode (PtCo/C TEC 36F62, Tanaka Kikinzoku Kogyo, Chiyoda, Tokio) for both MEA types. The loading was set on purpose to a level where fluctuations of the catalyst loading had no significant influence on MEAs' performances. The used gas diffusion layer (GDL) GDL 35 AI was sourced from SGL. The quality of the membrane–catalyst interface and a proper setting of the phosphoric acid content were the key features for MEA performance and durability [16,17]. Further information and details regarding the catalysts layer (CL) and assembly procedure cannot be specified due to the fact of proprietary issues.

2.2. Cell Compression Unit and Fuel Cell Test Station

At the DLR Institute of Networked Energy Systems in Oldenburg, commercially available compression units (CCUs) from balticFuelCells, Germany, were used. An exact and constant contact pressure (0.75 MPa) on the active MEAs, nominally 25 cm^2, was executed by an automated hydraulic piston of the CCUs. For the experiments shown here, serpentine flow fields (SFFs) were used with a land area of 13.4 cm^2 per side (cathode and anode); this led to an absolute pressure of 1.4 MPa [18].

The extended long-term tests at DLR, shown here, were carried out with an evaluator C1000-LT test bench by Fuel Con AG, Germany. Constant stoichiometry was chosen during the fuel cell tests. On the anode side, 1.3 for dry reformate (Ref.) (66% H_2, 11% N_2, 22% CO_2, and 1% CO (all Vol(%))) and 1.5 for pure hydrogen were selected. For the cathode gas supply, a stoichiometry factor of 2 was selected for air and 9.5 for pure oxygen. The cell temperature was kept constant at 160 °C by electrical heating through the CCU. The long-term tests were conducted for one year (8760 h) or until reaching end of life (EoL = 90% of the initial voltage value).

To implement this extended lifetime testing, the reformate constituents H_2, N_2, and CO were fed to the test bench via premixed bottles, and CO_2 was added from an existing plant. For the reformate bottles, a system with its own gas sensors was installed to be independent of the in-house supply. In addition, redundancies for N_2 (emergency flushing system), H_2, and pressurized air were integrated into the system. Pressurized air supplies were not only on the cathode side but also on the pressure control of the CCUs and actuators of the test bench itself. To prevent a shut-down of the experiment due to the fact of a power blackout, an uninterruptible power supply (PSG electronics PSG-120-20-5) was installed. Furthermore, the exhaust gas discharge from the in-house exhaust air system was made independent by a direct line out of the building. This ensured that the fuel cell test did not have to be stopped due to the presence of external influences.

The measurements at FUMATECH were carried out at a test station from Greenlight Innovation, Canada. The MEA was crimped in a holder of ElectroChem Inc. (Woburn, MA, USA), by eight screws each with a torque of 2.2 Nm in an area of 25 cm^2. In contrast to the test station at DLR, the test rig was not specially adapted for a long-term test because, as mentioned above, it was a measurement outside the QUALIFIX project. Another difference were the feed gases; FMT-C was run on the anode with pure hydrogen at a stoichiometry of 1.5 and a dew point of 70 °C. At the cathode, compressed air with different stoichiometries from 2.0 to 3.5 were used.

2.3. Fuel Cell Test Procedure

For FMT-A and FMT-B, The cells were heated at the beginning of the test to 120 °C under N_2 atmosphere. After reaching this temperature, the gases were changed to pure H_2 at the anode and air at the cathode side and heating up to 160 °C was continued. As soon as an open-circuit voltage was present, the electrical load was set stepwise to 0.3 A/cm^2, taking into account that the cell voltage does not drop below 0.3 V during the start-up process. As soon as the target temperature of 160 °C was reached, a 48 h start-up phase began. After this activation phase, a begin of life (BoL) electrochemical characterization with polarization curves, electrochemical impedance spectroscopy (EIS), cyclic voltammetry (CV), and linear sweep voltammetry (LSV) was performed [16,19,20]. The polarization curves and EIS were performed under H_2/air, H_2/O_2, Ref./O_2, and Ref./air; only a selection are presented within this publication. After the characterization, the anode gas was changed to the mentioned dry reformate. The characterization was repeated at the end of test (EoT) or end of life (EoL). In addition to the BoL and EoL/EoT characterizations, every 1000 h characterizations were performed. These were in the case of FMT-A being identical to that of BoL/EoL. For the second MEA (FMT-B), the characterizations were limited in order to protect the single cell; only a reduced polarization curve to 0.5 V and impedances with reformate were executed.

To perform the electrochemical measurements (EIS, CV, and LSV), an external potentiostate (Modulab 2100A, Solartron Analytical, Farnborough, United Kingdom) was connected to the CCU. The AC voltage for EIS measurements varied between 100 mHz and 100 kHz with an amplitude

perturbation of 10 mV root mean square (r.m.s). For the CV and LSV measurements, nitrogen was supplied at the working electrode (cathode) and pure hydrogen at the counter/pseudo reference electrode (anode) with 0.1 L/min each for the CV and 0.3 L/min each for the LSV. The CVs were performed with a scan rate of 100 mV/s between 0.05 and 1.0 V, while the LSV was swept with a rate of 2 mV/s between the initial value and 0.5 V.

For FMT-C, the operation of the cell started at room temperature under non-humidified hydrogen (stoichiometry 1.5 that met 5A) and compressed air (stoichiometry 2.0 that met 5 A). The temperature of the cell increased with a rate of approximately 4.5 °C/min. When the temperature approached 120 °C (i.e., approximately 22 min from the start of the operation when the cell was kept under open circuit voltages (OCV)), the current was drawn. The rate was manually controlled and was set to 0.2 A/min. At about 150 °C, the cell reached flow-wise steady-state conditions. After final temperature of 160 °C was approached, the cell was operated for about 120 h in a steady mode, and the polarization curve was recorded. After that, the chosen protocol was adopted.

2.4. Micro-Computed Tomography

The micro-computed X-ray tomograph Skyscan 1172 Desktop micro-CT (Bruker, Belgium) was used as the imaging procedure for all MEAs FMT-A, -B, and -C at the DLR. With the help of this device, a non-destructive examination of the MEA samples and a direct ante- and post-mortem comparison was possible. For this purpose, samples were punched out using a standard punching tool with a diameter of 4 or 8 mm, and these samples were scanned in the next step. During this CT scan, a large number of cross-sectional images, so-called radiographs, were recorded at different angles and subsequently assembled as computer-based 3D volume images. In Table 2, the setting of parameters used during the µ-CT scan are specified. Further information regarding this imaging procedure can be found in the literature [21].

The thickness values of the MEA layers, such as gas diffusion layers (GDLs), microporous layers (MPLs), catalyst layers (CLs), and membrane were calculated from a minimum of 10 values of five cross-sectional 2D images (sagittal and coronal), respectively, with help of the software DataViewer. This software was also used to create two-dimensional cross-sectional images. With help of the software CTVox (Bruker, version: 3.3.0 r1403), 3D images were generated.

Table 2. µ-CT (micro-computer tomography) operational parameters.

Parameter	Value
Acceleration voltage (kV)	79–82
Current (µA)	100
Sample size, Ø (mm)	4 (8 for FMT-C)
Rotation step (°)	0.2
Random movement	10
Averaging	4
Optical resolution (µm/px)	1.5–2.3
Duration (h)	2–4
Temperature (°C)	23–27

2.5. Detection of Phosphoric Acid

The determination of the phosphoric acid content within the MEAs was performed ante- and post-mortem for FMT-A and -B at the DLR but not for FMT-C, because this had to happen close to the end of the test, and this was logistically not feasible. For each tested MEA, three samples were cut with the help of a standard punching tool with a diameter of 8 mm. Separations of the single layers (GDL, CL, and membrane) were undertaken for every sample. Afterwards, these layers were stirred in a mixture of 70% distilled H_2O with 30% acetone for 30 min at room temperature. The next step was the removal of residual layer parts from the solution. Subsequently, the mixture was titrated with

0.1 M sodium hydroxide. Therefore, the automatic titrator TitroLine alpha plus (SI Analytics, Mainz, Germany) was utilized in order to determine the acid content.

3. Results and Discussion

As already described above, the execution of a complete single-cell annual test at a constant load of 0.3 A/cm^2 was one of the main tasks in the context of the project QUALIFIX. The first annual test was conducted with an MEA with Fumapem® AM-40 as the membrane and under reformate and air supply. This MEA is hereinafter referred to as FMT-A. Figure 1 shows the voltage gradient of this single cell (grey). Within the first 1000 operating hours, the voltage increased with at an average rate of 10 µV/h. One possible cause for the voltage exaltation after start-up could be that the full potential of the MEA was not reached, as it has already been observed several times [6,22]. After 1000 h of operation, as foreseen in the test protocol, the single cell was again completely characterized. The degradation increased in the following 1000 h of operation, so that a degradation rate of −3.5 µV/h was recorded over the total period of 2000 operating hours. In order to reduce the influence of the characterization on the test specimen degradation, the characterization of the MEA was shortened. Especially, the CV and LSV measurements burdened the MEA significantly more than the EIS or polarization curves under the given conditions. For all subsequent characterizations, with exception of the final characterization at the end of the test, the CV and LSV measurements were omitted; this resulted also in a shortened characterization after 2000 h of operating time for the FMT-A. From the ensuing voltage gradient, a rapid loss of voltage, starting directly after characterization, became clear. The average degradation rate from 2000 h of operation until EoL was approximately −80 µV/h. Due to the high degradation, the MEA reached the EoL threshold (EoL = initial voltage value – 10%) after approximately 700 additional operating hours. The rapid loss of voltage results from irreversible damage to the MEA which made further operation of the test specimen impossible. After 2600 h of operation, the intended annual test with FMT-A was completed with a full electrochemical characterization.

Due to the early EoL of the annual test of MEA FMT-A, a second annual test was started. For this purpose, an MEA with a Fumapem® AP-40 membrane was used. This MEA bears the name FMT-B in this publication. The associated voltage gradient is also shown in Figure 1 (green). It should be mentioned that the number of MEAs presented here in the comparison study cannot be judged as a statistical one. On the other hand, the measurements of performance as an initial hurdle suggest a systematic difference between Fumapem® AM and Fumapem® AP. It can be concluded that the interface of the electrode in the Fumapem® AP might have the more advantageous structure in terms of performance as shown in Figures 1 and 2d. What is noticeable in the direct comparison of FMT-A and -B, besides the short running time and the significantly higher degradation, is the considerably higher initial voltage value of the FMT-B, despite the same platinum loading of this MEA compared with FMT-A.

As can be clearly seen, the voltage of FMT-A increased even further after the start of the test and reaches a maximum of 0.646 V at a constant current density of 0.3 A/cm^2 within approximately 500 h of operation. The voltage increase could be due to the insufficient activation of the MEA during the start-up as already detected with MEA FMT-A. In comparison to FMT-A, the test procedure for FMT-B was adapted in some places in order to protect the MEA even more and to detect a material failure as early as possible. The characterization of the single cell, which is performed during the annual test every 1000 h of operation, was shortened. To keep the influence of the electrochemical characterization on the MEA degradation as small as possible, the characterization was reduced to polarization curves with dry reformate and air including the corresponding electrochemical impedance spectroscopy (EIS).

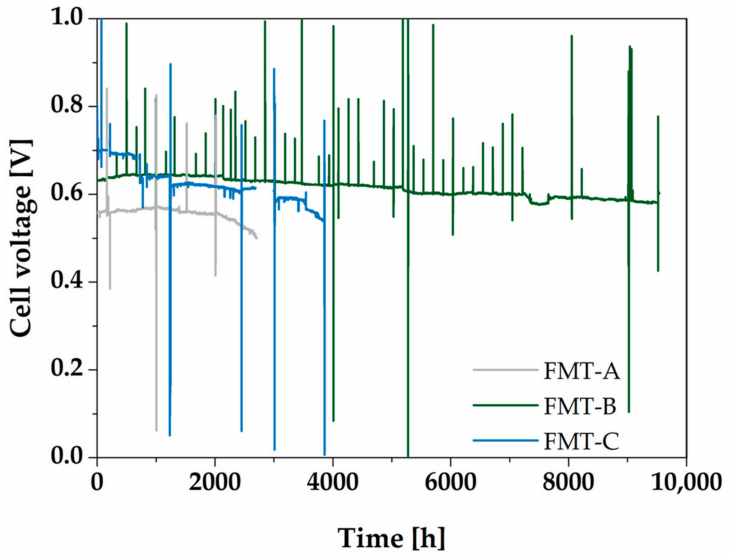

Figure 1. Fuel cell voltage as function of time under long-term test conditions with reformate and air (λ = 1.3/2.0) of FMT-A (grey), FMT-B (green), and FMT-C (blue) under constant load (0.3 A/cm^2), 160 °C.

Between 7000 and 8000 h of operation technical problems occurred which were due to the experimental setup and not to the MEA which showed a fairly stable behavior as can be seen in Figure 1. The significant drop in the voltage after 7100 h was due to the anode-side gas supply, where there was a narrowing of the gas supply line which resulted in a lower gas stream. This could be solved by a bypass and the MEA FMT-B was able to recover almost completely from this incident. The MEA FMT-B can be operated for over 9500 h under reformate supply without reaching EoL.

For FMT-C, a significantly higher voltage of 700 mV at the start of the test was noticeable. The reason for this was probably the use of pure hydrogen which, compared to FMT-A and -B, eliminates dilution by the gases N_2 and CO_2 and the effect of CO. The first significant voltage drop in the cell voltage after approximately 650 h was due to a failure of the test station. As a result, the MEA lingered at approximately 70 h at OCV which caused irreparable damage and is reflected in the voltage drop to 641 mV. The next recorded voltage reduction at approximately 1250 h was caused by a faulty supply of hydrogen. This fuel starvation also caused damage [23], causing the voltage to drop to 620 mV. From this incident, there was a slight regeneration [23] over the period up to approximately 1600 h to 625 mV but subsiding from here with a degradation rate of 23.3 µV/h to 604 mV after approximately 2450 h of operation. The subsequent increase to 612 mV can be attributed to an increase in the cathode stoichiometry from 2 to 3.5. This increase continued up to 614 mV until approximately 2700 h. In the following 300 h, the data are missing due to the fault of the test station but does not result in a test abort. After this time, the voltage dropped to 607 mV which is a degradation rate of 22.7 µV/h and very close to the rate at a stoichiometry of two. It can be concluded that the increase in the cathode flow had neither a positive nor negative effect on the MEA, since with increased flow, more phosphoric acid can also be discharged; this would have been an expected negative consequence. After a controlled shutdown for operational reasons, the test was continued again with a cathode stoichiometry of 2 (from 3000 h on). After a break-in phase, a significantly lower voltage was noticeable which stabilizes at 592 mV. If the abovementioned degradation rate were to continue from 2450 h (cathode stoichiometry = 2), the result would arithmetically be a value of 589 mV. It can be concluded that the degradation was constant from the period of 1600 h to 3100 h despite various influences and was caused by the same process. The last voltage drop, at about 3550 h, was due to the second undersupply of hydrogen. However, in this case, a larger amount to damage occurred which cannot be recovered from as shown by the drop in voltage to 540 mV at the end of the test after approximately 3840 h at a significantly increased degradation rate of 83.3 µV/h.

During the course of the test of the FMT-A, until 2000 h of operation, the performance steadily increased (see Figure 2a). The polarization curve at EoL after 2600 h of operation shows a distinctly reduced performance than the previous polarization curves which also corresponds to the significantly higher degradation rate (from 2000 h, see Figure 1) and a bend in the curve due to the higher stoichiometry, up to 0.06 A/cm^2, because of a mass flow controller which reinforces the H_2 crossover effect. The attrition of the OCVs, which is already recognizable after 1000 h, is striking. At the beginning of test, the OCV exhibited a value of 950 mV, but then it fell steadily. At 2600 h, an OCV of only 650 mV was reached. The open circuit voltage of the MEA was directly affected by the mixed potential losses in the current-free state. By diffusion of hydrogen and oxygen through the membrane, the direct reaction of the reactants without electron transport via load circuit occurred. The result was a reduction in the OCV. In practice, the flow of hydrogen was dominant due to the small molecular size. The illustrated decrease in the OCVs therefore indicates an increase in hydrogen crossover.

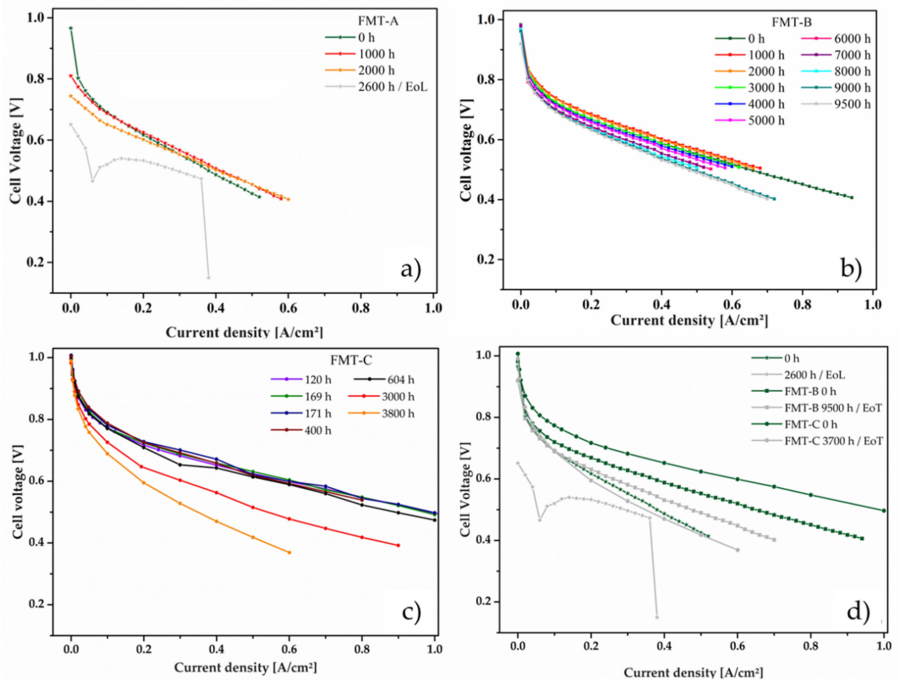

Figure 2. Polarization curves under dry reformate and air supply (λ = 1.3/2.0), recorded at begin of life BoL, end of test/end of life EoT/EoL and at certain intervals: (**a**) FMT-A, (**b**) FMT-B, (**c**) FMT-C, and (**d**) comparison of FMT-A, FMT-B, and FMT-C at BoL/EoL/EoT.

As previously described, the characterization for the MEA FMT-B was adjusted. Therefore, the polarization curves were performed up to a minimum voltage of 0.5 V, except the begin and end of tests; during the extended characterization (at 0, 9000, and 9500 h) the voltage threshold during the polarization curves went down to 0.4 V. In Figure 2b, these polarization curves are presented. During the first 2000 h of the long-term test, the FMT-B, like FMT-A, showed an increase in performance and, thus, represents an activation of the MEA. Subsequently, this MEA showed uniform and low-performance consumption which is also reflected in the low degradation rate (see Figure 1). In addition, there was hardly any decrease in the OCV values during the extended long-term test (see Figure 2b).

In Figure 2c, the polarization curves also showed no significant loss in the OCV for FMT-C. However, the fuel starvations left a clearly damaged MEA; this effect was further intensified by natural degradation.

In Figure 2d, the polarization curves for all three MEAs are compared. Both FMT-B and -C show a much better performance than FMT-A. It should be noted here, again, that FMT-A and -B were operating under reformate and FMT-C under pure but humidified hydrogen.

It is also important to note that, while the MEA FMT-A showed only 2600 h between the two polarization curves, the time difference for FMT-B adds up to 9000 h. Although a slight deterioration in performance was observed for FMT-B, the degradation for FMT-A was significantly higher. These observations confirmed the selection of the correct adaptations for FMT-B.

In addition to the polarization curves, electrochemical impedance spectra were recorded, and the results are shown in Figures 3 and 4. The values presented in Figure 4 were derived from the impedance measurements plots shown in Figure 3. The ohmic resistance was determined from the intersection in the high-frequency determined area [24]; in combination with the diameters of the semi-circles, the total resistance [25] was obtained. The results show that the ohmic resistance of FMT-A decreased by 0.1 Ω/cm^2 over the test duration of 2600 h (see Figure 4a,b). The noticeable decrease in ohmic resistance indicates a highly diluted membrane. In the case of MEA FMT-B, the decrease in ohmic resistance (from 0.58 to 0.53 Ω/cm^2) was only half as high compared to FMT-A over the complete test duration of >9000 h. This shows that despite the three times shorter test duration, the decrease in ohmic resistance was higher for FMT-A. This also shows the improvement in the membrane quality between FMT-A (Fumapem® AM-40) and FMT-B (Fumapem® AP-40) very clearly. One of the possible explanations is the poorer retention of phosphoric acid in the interface of the MEA using Fumapem® AM (FMT-A) which is observed during the long-time experiments. This is shown by the similar phosphoric acid contents of the EoL-MEAs as presented in Figure 5. However, the similarity of the EoL content was achieved after approximately 2500 h (AM) versus 10,000 h (AP).

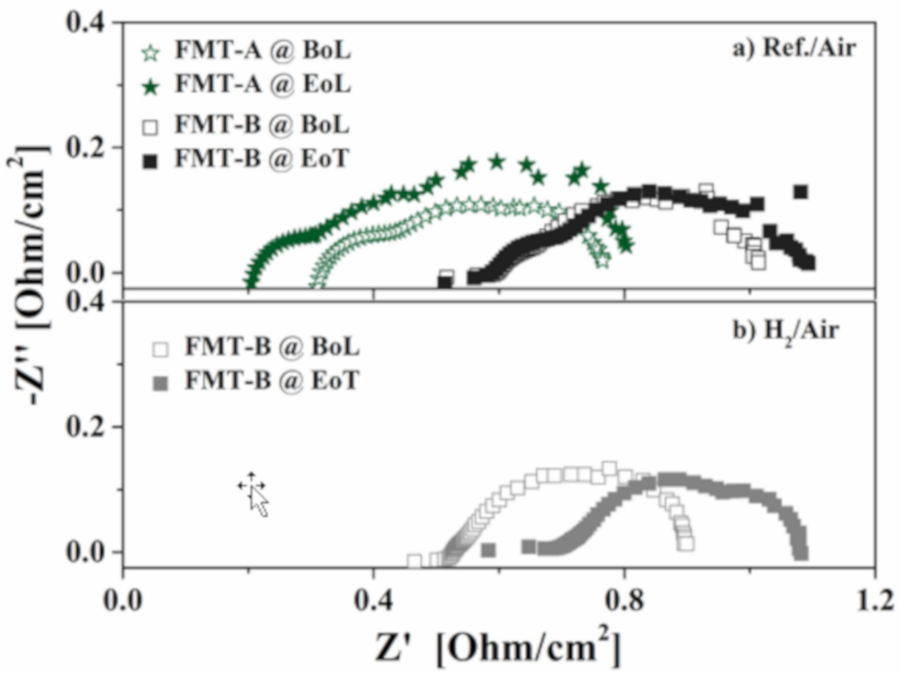

Figure 3. Nyquist plots of (**a**) FMT-A and FMT-B with fed of reformate/air (λ = 1.5/2) and (**b**) FMT-B with fed of H2/air (λ = 1.5/2) operated at BoL and EoL. The cells were operated at 160 °C and 1 atm under the current density of 0.3 A/cm^2. For FMT-A EoL was 2600 h and for FMT-B EoT was 9500 h.

The data for FMT-A under hydrogen at EoL are missing in Figure 4, because the deviation of the values was too large, hence measurement was not possible. One assumption is that, in the case of pure hydrogen, more gas passes through the damaged membrane in comparison to reformate gas, where the hydrogen is diluted. If one considers the change from reformate to hydrogen for FMT-B during the BoL examination (Figure 4), a decrease in the ohmic resistance under hydrogen operation is shown. One reason for the decrease could be the reduced volume flow in the case of hydrogen compared to the reformate supply. Due to the reduced volume flow when using hydrogen, less gas is available which can transport water from the MEA. This can therefore lead to a dilution of the electrolyte which, in turn,

improves the conductivity as already shown by Liu [26]. However, this explanation cannot be cited for the EoT observations shown in Figure 4b, since the ohmic resistance in this case rose when reformate was changed to hydrogen. This shows the complex reactions caused by the reformate operation and the degradation after more than 9000 h of continuous operation; these observations will have to be examined more closely and further in the future.

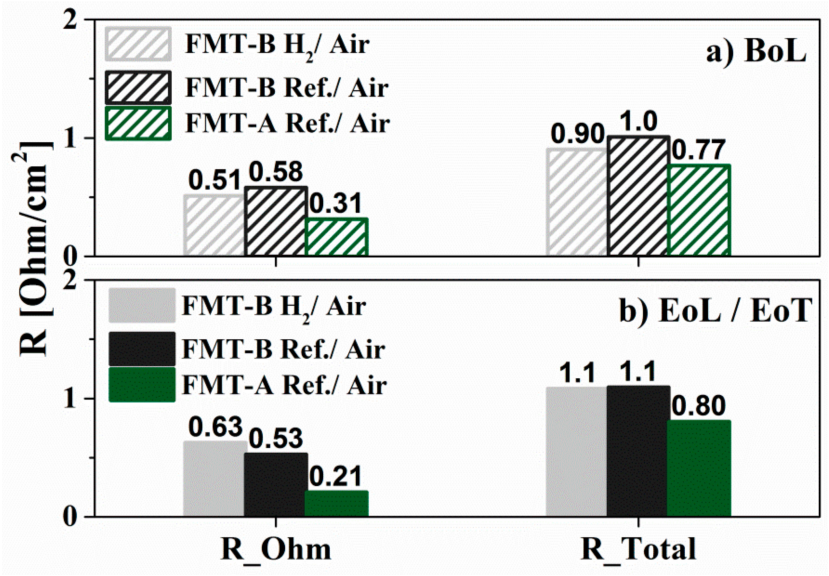

Figure 4. Ohmic resistance (R_Ohm), total resistance (R_Total), and the ratio of them (R_Ohm/Total) of FMT-A and FMT-B calculated from Figure 3.

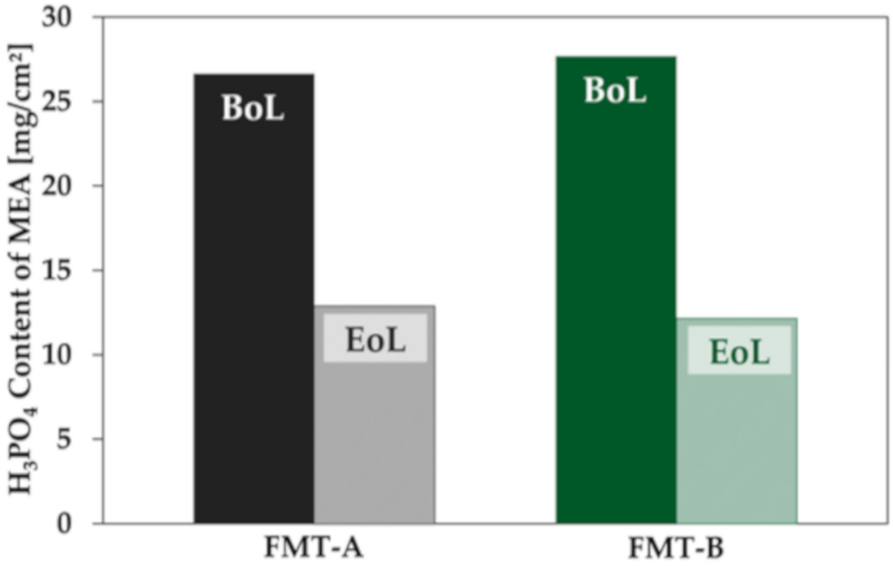

Figure 5. H_3PO_4 content of FMT-A and B before (BoL) and after long-term test (EoL) at 0.3 A/cm^2.

The determination of the ohmic resistance for the two MEAs FMT-A and FMT-B indicates a distinctly different degradation behavior of the two membrane types. For this reason, the H_2 crossover and the internal short circuit resistance were also determined with the help of LSV measurements, and the results are presented in Figure 6. Due to the different test protocols, such a measurement was not carried out with FMT-C.

In the case of FMT-A (see Figure 6), the hydrogen crossover increased significantly over the 2600 hours of operation. A crossover current of approximately 4 mA/cm^2 was detected at the start of the test. After 1000 h of operation, the current increased to approximately 30 mA/cm^2 and reached a

maximum of 200 mA/cm^2 at 2600 h. At the same time, the internal resistance of the MEA decreased similarly. After 2600 h, the internal short circuit resistance fell from the initial 10 Ω to nearly 0 Ω. All the results of electrochemical characterization indicate possible damages of the membrane which could be the cause of the cell failure. In terms of hydrogen crossover, the MEA FMT-B showed quite a different behavior in direct comparison with the FMT-A: FMT-B showed a very low and also stable hydrogen crossover current in the course of the experiment, while the FMT-A, as described above, had a similar starting value but increased significantly over the course of the considerably shorter test. In addition, the internal short circuit resistance of FMT-B decreased by 50%. While the constant hydrogen crossover is an indicator of a defect-free membrane, the reduction of the internal short circuit resistance is a sign of a possible thinning of the membrane [27].

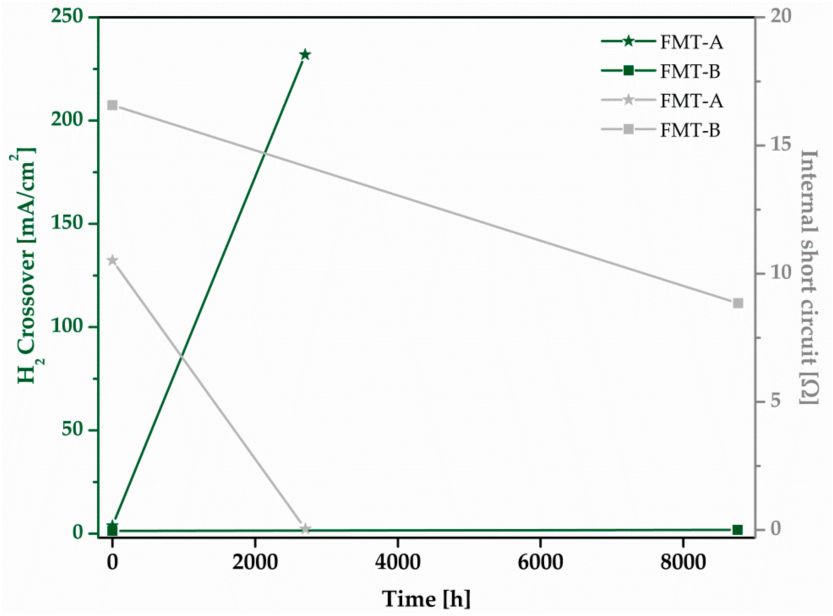

Figure 6. H_2 crossover and internal short circuit of FMT-A and FMT-B calculated from LSV measurements, BoL, and EoL/EoT.

Due to the assumptions of a destroyed membrane in the case of MEA FMT-A and a thinned membrane within FMT-B based on the electrochemical investigations presented above, the MEAs were examined by post-mortem analysis with help of µ-CT investigations and compared with the respective untested reference MEA from the same batches. In Figure 7a, the ante-mortem test results of the reference MEA to FMT-A (hereinafter referred to as BoL) are shown, and Figure 7b represents the results of the post-mortem analysis of the FMT-A after 2600 h under constant load operation. Because the BoL-MEA was not hot pressed, the MEA was delaminated, while the tested MEA FMT-A could be scanned as one because of the compression force within the Baltic CCU.

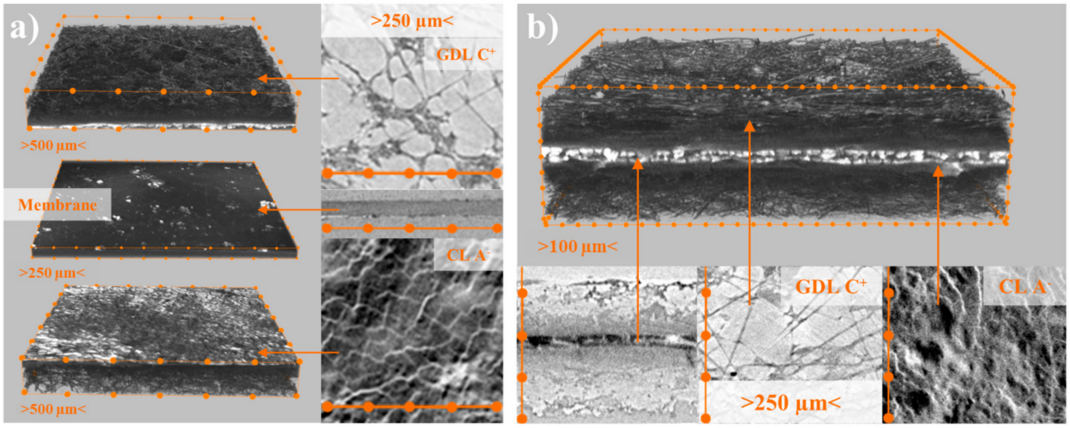

Figure 7. Reconstructed 3D images (CTVox) of the complete MEA: (**a**) FMT-A BoL and (**b**) FMT-A. Zoom-in areas are reconstructed 2D images (DataViewer) of single layers (GDL, Membran, CL).

In a direct comparison, it is clear to see how severe the MEA was degraded after 2600 h of operation at a constant load. The membrane, which is well recognizable in the reference MEA, showed uniform layer thicknesses and no defects as can be seen clearly in Figure 7a, is almost completely destroyed after operation. One reason for the destruction of the PBI membrane might be oxidative degradation due to the incomplete reduction of O_2 on the cathode (C^+) which leads to the generation of hydroperoxyl and hydroxyl radicals [28,29]. The catalyst layers, anodic and cathodic, are directly adjacent to each other and, thus, provide the reason for the high hydrogen crossover (Figure 6), the decrease of ohmic resistance (Figures 3 and 4), and the reduction of the internal short circuit resistance to 0 Ω. What is striking, when looking at the catalyst layer, is that this layer is covered by many fine hairline cracks (Figure 7a,b). This is also the case for the post-mortem observation; there is hardly a further expanding of the drying cracks, as it can be seen within the two 2D zoomed-in images of both MEAs. The layer thickness analysis also clearly shows (see Table 3) that the other layers hardly show any changes, a slight overall decrease on the anode (A^-) side, but the failure of the MEA FMT-A is almost entirely attributable to the membrane.

Table 3. Average layer thicknesses of FMT-A BoL and FMT-A determined by DataViewer.

Layer	Average Layer Thickness and Standard Deviation (µm)	
	Reference MEA (FMT-A BoL)	**FMT-A**
GDL Cathode	187 ± 17	183 ± 13
MPL Cathode	124 ± 13	112 ± 8
CL Cathode	57 ± 17	44 ± 4
Membrane	75 ± 6	destroyed
CL Anode	35 ± 7	33 ± 6
MPL Anode	100 ± 11	127 ± 13
GDL Anode	261 ± 31	200 ± 27
Total	delaminated	684 ± 22

Figure 8 shows the µ-CT studies of the MEA FMT-B (Figure 8b) which exceeded the long-term test. A direct comparison with an untested MEA from the same batch was also mentioned here (Figure 8a). A slight delamination could be also observed for the reference MEA, but it was possible to scan the MEA as one. The MEA FMT-B was delaminated while removing it from the CCU.

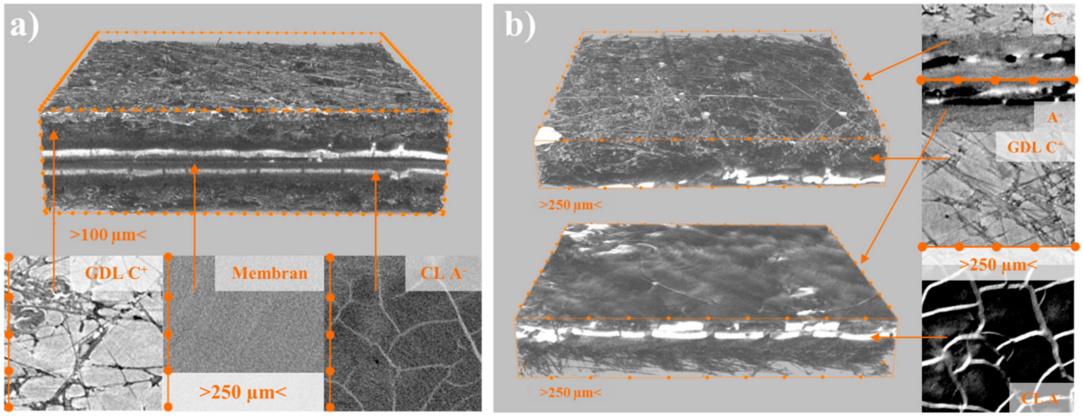

Figure 8. Reconstructed 3D images (CTVox) of the complete MEA: (**a**) FMT-B BoL and (**b**) FMT-B. Zoomed-in areas are reconstructed 2D images (DataViewer) of single layers (GDL, Membran, CL).

Also in the case of the FMT-B, with the help of this imaging method, a statement made by the electrochemical measurements could be substantiated. The thinning of the membrane after more than one year of running time could be confirmed by µ-CT investigations as shown in Figure 8b, and Table 4 confirms that the membrane shrunk from just under 60 µm to 21 µm and, thus, has only a third of the starting thickness. Furthermore, it can be observed that the drying cracks in the catalyst layer widened significantly in the course of the experiment as shown in Figure 8a,b). The chosen test conditions seem to indicate structural changes in the CL [30] for both MEA types (see Figures 6 and 7). Similar observations were made by Pokhrel at al. [31]; the slight drying cracks, due to the manufacturing process, within the BoL-CL also widened significantly, even more so, the CL exhibit an island structure. This could be due to the dehydration of the catalyst layer or bulk carbon corrosion [32]. But, as mentioned above in the Section 2, the catalyst loading was chosen to be significantly higher (e.g., on the cathode 1.6–1.7 mg/cm^2 where values of 1 mg/cm^2 are common [33]) to avoid significant influences by the catalyst degradation. This can be shown for FMT-B, since it was possible to quantify the loss of Pt ESA by cyclovoltammetry. The values for FMT-B showed a Pt ESA loss of 34% which is an acceptable value considering the very long test duration of 9800 h. Measurements with MEAs of similar performance show a loss of 12%–20% already after 500 h [11].

Table 4. Average layer thicknesses of FMT-B BoL and FMT-B determined by DataViewer.

Layer	Average Layer Thickness and Standard Deviation (µm)	
	Reference MEA (FMT-B BoL)	**FMT-B**
GDL Cathode	196 ± 11	165 ± 12
MPL Cathode	108 ± 6	116 ± 9
CL Cathode	46 ± 5	54 ± 11
Membrane	59 ± 7	21 ± 3
CL Anode	45 ± 5	35 ± 6
MPL Anode	115 ± 10	123 ± 11
GDL Anode	132 ± 13	149 ± 15
Total	735 ± 13	delaminated

For FMT-C, similar statements can be made as for FMT-B regarding the membrane (Figure 9). Due to the circumstances of the measurement, there is no BoL Image of the MEA FMT-C. Assuming, however, that the thickness was initially at 60 microns as for FMT-B, the EoT value of 40 microns (see Table 5) is comparable to the rate of thinning over time for FMT-B. Striking is the strong decrease of the CL layer on the anode and the adhesion of this layer to the membrane. These facts support the abovementioned assumption that the process of anode starvation was responsible for a main part of the degradation as observed by Yezerska et al. [23].

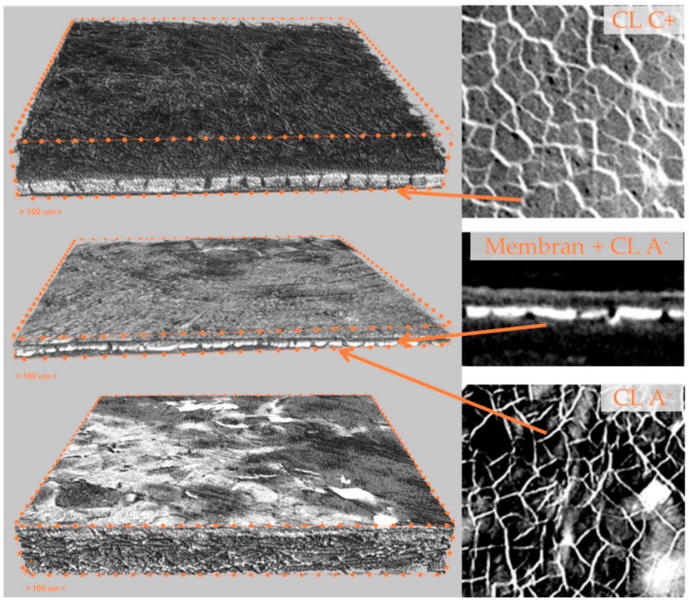

Figure 9. Reconstructed 3D images (CTVox) of the complete MEA FMT-C EoT. Zoomed in areas are reconstructed 2D/3D images (DataViewer) of single layers (GDL, Membran, CL).

Table 5. Average layer thicknesses of FMT-B BoL and FMT-C determined by DataViewer.

Layer	Average Layer Thickness and Standard Deviation (µm)	
	Reference MEA (FMT-B BoL) from Table 4	FMT-C
GDL Cathode	196 ± 11	114 ± 6
MPL Cathode	108 ± 6	69 ± 7
CL Cathode	46 ± 5	40 ± 4
Membrane	59 ± 7	40 ± 2
CL Anode	45 ± 5	21 ± 4
MPL Anode	115 ± 10	65 ± 4
GDL Anode	132 ± 13	117 ± 6
Total	735 ± 13	delaminated

Figure 5 shows the H_3PO_4 contents of the tested MEA before (solid pillar) and after (striped pillar) the two long-term tests at a constant load of 0.3 A/cm^2. Although the MEAs were equipped with different membranes, the phosphoric acid content was similar before and after the respective tests.

Figure 10 shows an alternative method for determining the phosphoric acid content of FMT-C. Since, as mentioned above, no such measurement could be performed for this MEA. The data shown here from a dynamic mechanical analysis (DMA) performed at FUMATECH show an example of an MEA/membrane of the same membrane chemistry after 1000 h (FMT-X) operation compared with FMT-C after EoT (3850 h). The significantly increased modulus of elasticity for FMT-C shows a higher strength of the membrane. From this, one can deduce an increased rigidity of the membrane which is an indication of the loss of phosphoric acid. This fact reinforces the suspicion that the membrane, as confirmed by FMT-B by determining the H_3PO_4 content, thinned due to the phosphoric acid loss. However, a direct comparison between FMT-B and -C shows that this fact does not lead to a failure of the MEA which speaks in favor of the AP membrane chemistry.

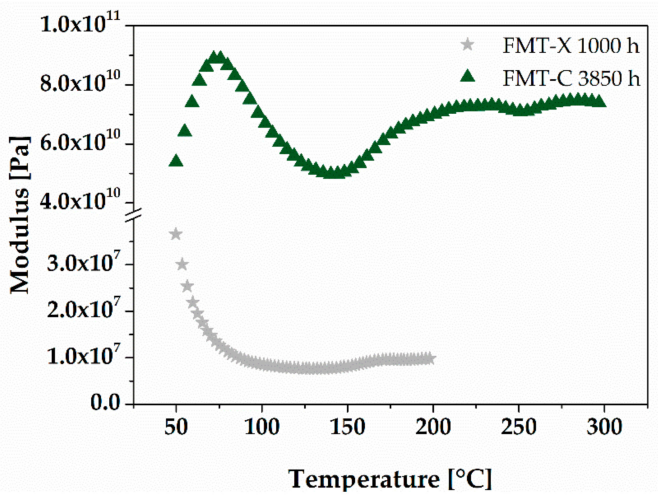

Figure 10. Dynamic properties of FMT-C after EoT (3850 h) and a MEA (FMT-X) of the same membrane chemistry after 1000 h operation.

The different methods for determining the phosphoric acid content demonstrate that FUMATECH has managed to ensure a uniform doping for the membranes over different batches and MEA types. This also shows that, in this case, the H_3PO_4 content can be removed from the degradation effect analysis, although phosphoric acid loss is one of the driving degradation paths [34]. However, in a direct comparison of the BoL- and EoL-H_3PO_4 contents of FMT-A and -B, it is noticeable that in both cases, the phosphoric acid concentration within the MEA was reduced by almost 50%. This observation agrees with the hypothesis made by Oono [35] that a low thinning rate of the membrane is associated with a low phosphoric loss rate because of the high H_3PO_4 loss is in conjunction with the destruction of the membrane of FMT-A and the thinning of the membrane by two-thirds in the case of the MEA FMT-B and one-third for FMT-C (see also Reference [6]).

4. Conclusions

With the help of the studies shown here, it was possible to show that FUMATECH succeeded in developing a new and improved MEA in the course of the project QUALIFIX which can reach a duration of 10,000 h of operation. The decisive factor here was the use of an improved membrane which also exhibits significant thinning during the test course of more than one year under reformate and air gas supply. In addition, the comparison with the literature showed that the degradation depends not only on the material used, here membranes and also CL, but also on the operating conditions, since the MEAs, which were investigated by Søndergaard et al. [6] or Pokhrel et al. [31], were provided by completely different providers than those shown here.

Author Contributions: Conceptualization, J.B.; Data curation, J.B., M.R., K.R. and H.S.; Formal analysis, J.B., M.R. and H.S.; Methodology, T.K.; Project administration, P.W.; Supervision, A.D.; Writing – original draft, J.B. and M.R.; Writing – review & editing, T.K., K.R., H.S., P.W. and A.D. All authors have read and agreed to the published version of the manuscript.

Funding: This research was funded by the German Federal Ministry for Economic Affairs and Energy (BMWi) within the project QUALIFIX grant number 03Et6046A.

Conflicts of Interest: The authors declare no conflict of interest.

References

1. Wang, Y.; Chen, K.S.; Mishler, J.; Cho, C.S.; Adroher, X.C. A review of polymer electrolyte membrane fuel cells: Technology, applications, and needs on fundamental research. *Appl. Energ.* **2011**, *88*, 981–1007. [CrossRef]
2. de Bruijn, F.A.; Dam, V.A.T.; Janssen, G.J.M. Review: Durability and degradation issues of PEM Fuel Cell components. *Fuel Cells (Weinh. Ger.)* **2008**, *8*, 3–22. [CrossRef]

3. Yu, S.; Xiao, L.; Benicewicz, B.C. Durability studies of PBI-based High Temperature PEMFCs. *Fuel Cells (Weinh. Ger.)* **2008**, *8*, 165–174. [CrossRef]
4. Schmidt, T.J.; Baurmeister, J. Durability and reliability in high-temperature reformed hydrogen PEFCs. *ECS Trans.* **2006**, *3*, 861–869.
5. Oono, Y.; Sounai, A.; Hori, M. Long-term cell degradation mechanism in high-temperature proton exchange membrane fuel cells. *J. Power Sour.* **2012**, *210*, 366–373. [CrossRef]
6. Søndergaard, T.; Cleemann, L.N.; Becker, H.; Aili, D.; Steenberg, T.; Hjuler, H.A.; Seerup, L.; Li, Q.; Jensen, J.O. Long-term durability of HT-PEM fuel cells based on thermally cross-linked polybenzimidazole. *J. Power Sour.* **2017**, *342*, 570–578. [CrossRef]
7. Jeppesen, C.; Polverino, P.; Andreasen, S.J.; Araya, S.S.; Sahlin, S.L.; Pianese, C.; Kær, S.K. Impedance characterization of high temperature proton exchange membrane fuel cell stack under the influence of carbon monoxide and methanol vapor. *Int. J. Hydrog. Energy* **2017**, *42*, 21901–21912. [CrossRef]
8. Quartarone, E.; Angioni, S.; Mustarelli, P. Polymer and Composite Membranes for Proton-Conducting, High-Temperature Fuel Cells: A Critical Review. *Materials* **2017**, *10*, 687. [CrossRef]
9. Rastedt, M.; Büsselmann, J.; Tullius, V.; Wagner, P.; Dyck, A. Rapid and Flash Tests: Indicator for Quality of HT-PEM Fuel Cells Batches? *Fuel Cells* **2018**, *18*, 113–122. [CrossRef]
10. Rastedt, M.; Tullius, V.; Büsselmann, J.; Schonvogel, D.; Wagner, P.; Dyck, A. Evaluation of HT-PEM Fuel Cells via Load Cycling at High Current Densities. *ECS Trans.* **2017**, *80*, 3–17. [CrossRef]
11. Büsselmann, J.; Rastedt, M.; Tullius, V.; Yezerska, K.; Dyck, A.; Wagner, P. Evaluation of HT-PEM MEAs: Load cycling versus start/stop cycling. *Int. J. Hydrog. Energy* **2018**. [CrossRef]
12. Siegel, C.; Bandlamudi, G.; Heinzel, A. Modeling Polybenzimidazole/Phosphoric Acid Membrane Behaviour in a HTPEM Fuel Cell. In Proceedings of COMSOL 2008, Hannover, Germany, 4–6 November 2008; p. 7.
13. Cheddie, D.; Munroe, N. Parametric model of an intermediate temperature PEMFC. *J. Power Sour.* **2006**, *156*, 414–423. [CrossRef]
14. *Technical Data Sheet-fumapem® AM-40*; Fumatech BWT GmbH: Bietigheim-Bissingen, Germany, 2015.
15. *Technical Data Sheet-fumapem® AP-30*; Fumatech BWT GmbH: Bietigheim-Bissingen, Germany, 2015.
16. Beer, C.d.; Barendse, P.S.; Pillay, P.; Bullecks, B.; Rengaswamy, R. Classification of High-Temperature PEM Fuel Cell Degradation Mechanisms Using Equivalent Circuits. *IEEE Trans. Ind. Electron.* **2015**, *62*, 5265–5274. [CrossRef]
17. Wang, C.; Wang, S.; Peng, L.; Zhang, J.; Shao, Z.; Huang, J.; Sun, C.; Ouyang, M.; He, X. Recent Progress on the Key Materials and Components for Proton Exchange Membrane Fuel Cells in Vehicle Applications. *Energies* **2016**, *9*, 603. [CrossRef]
18. Diedrichs, A.; Rastedt, M.; Pinar, J.F.; Wagner, P. Effect of Compression on the Performance of a HT-PEM Fuel Cell. *J. Appl. Electrochem.* **2013**, *43*, 1079–1099. [CrossRef]
19. Pinar, F.J.; Rastedt, M.; Pilinski, N.; Wagner, P. Effect of Compression Cycling on Polybenzimidazole-based High-Temperature Polymer Electrolyte Membrane Fuel Cells. *Fuel Cells* **2015**, *15*, 140–149. [CrossRef]
20. Diedrichs, A.; Wagner, P. Performance Analysis of a High-Temperature Polymer Electrolyte Membrane Fuel Cell under Mechanical Compression Control. *ECS Trans.* **2012**, *50*, 1137–1153. [CrossRef]
21. Pinar, F.J.; Rastedt, M.; Pilinski, N.; Wagner, P. Characterization of HT-PEM Membrane-Electrode-Assemblies. In *High Temperature Polymer Electrolyte Fuel Cells-Approaches, Status and Perspectives*; Springer: Berlin/Heidelberg, Germany, 2016.
22. Rastedt, M.; Pinar, F.J.; Pilinski, N.; Dyck, A.; Wagner, P. Effect of Operation Strategies on Phosphoric Acid Loss in HT-PEM Fuel Cells. *ECS Trans.* **2016**, *75*, 455–469. [CrossRef]
23. Yezerska, K.; Dushina, A.; Liu, F.; Rastedt, M.; Wagner, P.; Dyck, A.; Wark, M. Characterization methodology for anode starvation in HT-PEM fuel cells. *Int. J. Hydrog. Energy* **2019**, *44*, 18330–18339. [CrossRef]
24. Barsoukov, E.; Macdonald, J. *Impedance Spectroscopy: Theory, Experiment, and Applications*; Wiley-VCH: Weinheim, Germany, 2005; p. 595.
25. Kim, J.-R.; Yi, J.S.; Song, T.-W. Investigation of degradation mechanisms of a high-temperature polymer-electrolyte-membrane fuel cell stack by electrochemical impedance spectroscopy. *J. Power Sour.* **2012**, *220*, 54–64. [CrossRef]
26. Liu, F. Interaction of phosphoric acid with cell components in high temperature polymer electrolyte fuel cells. PhD Thesis, RWTH Aachen, Aachen, Germany, 26 May 2014.

27. Aili, D.; Jensen, J.O.; Li, Q. Polybenzimidazole Membranes by Post Acid Doping. In *High Temperature Polymer Electrolyte Membrane Fuel Cells-Approaches, Status, and Perspectives*, 1st ed.; Li, Q., Aili, D., Hjuler, H.A., Jensen, J.O., Eds.; Springer International Publishing: Basel, Switzerland, 2016; pp. 195–215.
28. Liu, G.; Zhang, H.; Hu, J.; Zhai, Y.; Xu, D.; Shao, Z. Studies of performance degradation of a high temperature PEMFC based on H3PO4-doped PBI. *J. Power Sour.* **2006**, *162*, 547–552. [CrossRef]
29. Guo, Q.; Pintauro, N.P.; Tang, H.; O'Connor, S. Sulfonated and crosslinked polyphosphazene-based proton-exchange membranes. *J. Membr. Sci.* **1999**, *154*, 175–181. [CrossRef]
30. Kneer, A.; Jankovic, J.; Susac, D.; Putz, A.; Wagner, N.; Sabharwal, M.; Secanell, M. Correlation of Changes in Electrochemical and Structural Parameters due to Voltage Cycling Induced Degradation in PEM Fuel Cells. *J. Electrochem. Soc.* **2018**, *165*, F3241–F3250. [CrossRef]
31. Pokhrel, A.; El Hannach, M.; Orfino, F.P.; Dutta, M.; Kjeang, E. Failure analysis of fuel cell electrodes using three-dimensional multi-length scale X-ray computed tomography. *J. Power Sour.* **2016**, *329*, 330–338. [CrossRef]
32. Kundu, S.; Fowler, M.W.; Simon, L.C.; Grot, S. Morphological features (defects) in fuel cell membrane electrode assemblies. *J. Power Sour.* **2006**, *157*, 650–656. [CrossRef]
33. Zeis, R. Materials and characterization techniques for high-temperature polymer electrolyte membrane fuel cells. *Beilstein J. Nanotechnol.* **2015**, *6*, 68–83. [CrossRef]
34. Rosli, R.E.; Sulong, A.B.; Daud, W.R.W.; Zulkifley, M.A.; Husaini, T.; Rosli, M.I.; Majlan, E.H.; Haque, M.A. A review of high-temperature proton exchange membrane fuel cell (HT-PEMFC) system. *Int. J. Hydrog. Energy* **2017**, *42*, 9293–9314. [CrossRef]
35. Oono, Y.; Sounai, A.; Hori, M. Prolongation of lifetime of high temperature proton exchange membrane fuel cells. *J. Power Sour.* **2013**, *241*, 87–93. [CrossRef]